

Controlling the nucleation environment of *c*-BN films and their related properties

Quan Li,* L. D. Marks,* Y. Lifshitz,[†] S. T. Lee, and I. Bello[†]

*Center of Super-Diamond and Advanced Films (COSDAF) & Department of Physics and Materials Science,
City University of Hong Kong, Kowloon, Hong Kong, China*

(Received 22 May 2001; published 7 January 2002)

Cubic boron nitride (*c*-BN) films were deposited using radio-frequency (rf) magnetron sputtering. A type of turbostratic boron nitride (*t*-BN) growth was found by reducing the substrate bias during deposition. Transmission electron microscopy (TEM) study showed that the *t*-BN served as a different nucleation environment for *c*-BN compared to those reported in the literature by many other groups. The nucleation environment corresponded to a lower film internal stress level and thus facilitated the production of thicker *c*-BN films. The fraction of different *t*-BN/*c*-BN environments could be controlled and altered by varying the deposition conditions. The films containing different *t*-BN/*c*-BN environments were compared in phase concentration, stoichiometry, microstructure, and internal stress level. Additional insight was added to the film growth mechanism.

DOI: 10.1103/PhysRevB.65.045415

PACS number(s): 68.37.Lp, 68.55.Ac, 68.55.Ln, 61.30.Hn

I. INTRODUCTION

Cubic boron nitride is an excellent candidate for a variety of applications. For specific applications such as hard protective coatings, *c*-BN is superior to diamond due to its unique set of properties including high hardness second only to that of diamond and chemical inertness with Fe and Fe-based alloys at high temperatures. However, the thickness required for protective coating should be greater than 0.5 micron. Ion beam and ion-assisted techniques^{1–8} are able to produce ~100% *c*-BN. The nucleation of *c*-BN follows the sequential formation of first amorphous boron nitride (*a*-BN) and then oriented *t*-BN, on top of which *c*-BN nucleates, oriented to the *t*-BN and thus to the substrate. The *t*-BN layer grows with its (0002) basal planes perpendicular to the Si substrate. The *c*-BN seems to nucleate on the edge of the *t*-BN (0002) planes and further grow with its (111) planes parallel to the *t*-BN (0002) planes.^{1,7} This type of *c*-BN growth is associated with significant compressive stress, which is formed by the energetic ion impact. The compressive stress in the film limits the maximal thickness of these films to ~200 nm, beyond which cracking and delamination occurs. Much effort^{8–10} has been made to reduce the stress level in the *c*-BN films including the reduction of the bias either throughout the entire deposition scheme or after the *c*-BN nucleation commenced. The successful efforts combine the reduced bias with a high deposition temperature, so that the ion energy and the thermal annealing effects cannot be separated. These efforts aim at the deposition of thicker films. Intensive ion bombardment is nevertheless still applied to ensure *c*-BN nucleation. The stress levels in most of *c*-BN films exceed 5 GPa, which is too high for thick film growth.

In the present work, we report the existence of another *c*-BN nucleation environment. Curled *t*-BN (0002) planes were formed without any distinct orientation relationship to the Si substrate. *c*-BN nucleated on these curled *t*-BN planes grows in an disoriented manner relatively to the Si substrate, reducing the stress evolution. Moreover, by varying the deposition conditions, we show that the fraction of this type

of *t*-BN/*c*-BN nucleation environment can be gradually increased, reducing the stress in the film and enabling the growth of thicker films without delamination. We also give some additional insight into the *c*-BN nucleation process.

II. EXPERIMENTS

Boron nitride thin films were deposited in a Kurt J. Lesker rf magnetron sputtering deposition system, which had been described elsewhere.¹¹ The sputter target was a 99.99% pure hexagonal boron nitride disk of one inch in diameter. The base pressure in the deposition chamber was normally on the order of 10^{-9} Torr (a pressure of 10^{-7} Torr was found detrimental to *c*-BN growth, in accord with previous works¹²). The films were grown in a 50% Ar/50% N₂ mixture, which was one of the important conditions giving rise to stoichiometric BN films. The total pressure during deposition was kept at 10 mTorr to maintain a stable plasma. Silicon (100) wafers were used as substrates. They were first ultrasonically cleaned in acetone and methanol, and subsequently etched in a hydrofluoric acid solution in order to remove their native oxides and blow dried with dry nitrogen. Such hydrogen-passivated substrates were loaded into a load-lock chamber and then transferred into the deposition chamber. Prior to the deposition the silicon substrates were sputter-cleaned in an argon atmosphere at $\sim 10^{-2}$ Torr for 5 min in order to remove residual surface contaminants. The deposition temperature was maintained at 450 °C, controlled by a halogen-lamp heater. A high frequency pulsed dc bias at 333 kHz was applied to the substrate during deposition. The induced dc bias voltage varied from -50 to -120 V.

Cross-sectional transmission electron microscopy (XTEM) was used to investigate the microstructure of BN films. High-resolution images were taken by a CM 200 Philips microscope operating at 200 kV to characterize cross sectional samples. The *t*-BN and *c*-BN thickness of films with a sharp interface between the two phases could be determined with a resolution of 1 nm. Transmission electron diffraction (TED) patterns were taken using a Hitachi HF-2000 microscope operating at 200 kV. A Gatan GIF 200 at-

tached to the CM 200 microscope was used to perform electron energy loss spectroscopy (EELS), which monitors the bonding state of the films and distinguishes different BN phases. A 10 nm diameter electron beam operated in the diffraction mode was used to provide the structural information on the material confined in that region. By moving the electron beam along the film growth direction, the starting point of the *c*-BN nucleated on top of the *t*-BN was determined with a resolution of 10 nm, and the *t*-BN and *c*-BN film thickness were assessed for films where the interface between the *c*-BN and *t*-BN layers was not so sharp. The energy resolution was ~ 1 eV. Fourier transform infrared spectroscopy (FT-IR 1600, Perkin-Elmer) was used in the conventional way¹ to characterize the phase content in both transmission and reflection modes in the 700–1600 cm^{-1} wave number range. The background spectrum of an uncoated Si substrate was subtracted from each spectrum. The chemical composition of the films were examined by an x-ray photoelectron spectroscopy (XPS) using a VG ESCA LAB 220i-XL system equipped with a monochromatic Al $K\alpha$ x-ray source operating at 1486.6 eV photon emission. The internal stress of the film was evaluated from the Stoney equation¹³ by measuring the curvature of the Si wafer after film deposition, using a Tencor alpha step 500 profilometer.

III. RESULTS

Two types of boron nitride films designated (a) and (b) types were prepared by rf magnetron sputtering from a solid *h*-BN target. The film type (a) has been grown at the deposition conditions previously described using a substrate bias of -120 V. The maximum thickness of the film type (a) before its delamination is 100 nm. The internal stress of this film type (100 nm thick) is measured at ~ 11 GPa. XPS analysis shows a stoichiometric BN composition with residual O and C concentrations less than 3 and 2%, respectively. The film type (b) has been grown at the same deposition conditions as for the film type (a), but with a substrate bias of -50 V. The maximum thickness of the film type (b) before its delamination is 500 nm. The internal stress of the film type (b) (500 nm thick) is ~ 4.5 GPa.

Figure 1(a) shows a FTIR spectrum of the film type (a). The peak at 1075 cm^{-1} corresponds to the cubic BN phase, while the two peaks at 1370 and 780 cm^{-1} designate the hexagonal BN phase. The *c*-BN fraction of this film is calculated to be 84% using the conventional way.¹ Figure 1(b) represents a FTIR spectrum taken from the film type (b). The peak corresponding to the *c*-BN phase shifts from 1075 to 1065 cm^{-1} indicating a lower stress in the film (b) compared to film (a). The *c*-BN fraction in the film type (b) is calculated to be 63%.¹

Figures 2(a) and 2(b) are low magnification XTEM images of film type (a) and (b), respectively. Both images show layered contrast in the BN films. Within each XTEM image, the areas of interest, as designated in Fig. 2, were selected for the EELS analysis. The EELS spectra are presented in Fig. 3. The near-edge structure of the *B K* edge spectra (Fig. 3) consists of a sharp π^* peak, a broad σ^* peak, and an additional sharp peak.¹ The spectrum collected from the area 1 is

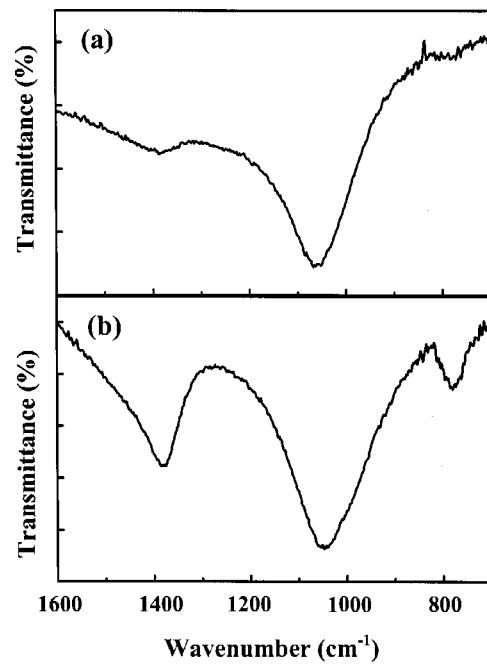


FIG. 1. FTIR spectrum of two BN films deposited using a power of 75 W on silicon substrate at 450 °C. The film (a) (100 nm thick) was deposited using a substrate bias of -120 V. The film (b) (500 nm thick) was deposited using a substrate bias of -50 V.

characteristic with a strong π^* peak at 191 eV arising from the sp^2 bonded BN. However, the π^* peak in the spectrum from the area 2 and above is absent, and an additional sharp peak appears next to the σ^* peak indicating that the BN phase in the film type (a) above the area 2 is practically 100% *c*-BN. The EELS analysis of the films (b) in the area 3 and region below, close to the substrate interface, also reveals a strong π^* peak due to the sp^2 bonded BN. The area 4 gives a similar spectrum to that taken from the area 3, but with a reduced relative intensity of the π^* peak. The spectra accumulated from the regions, which are more apart from the

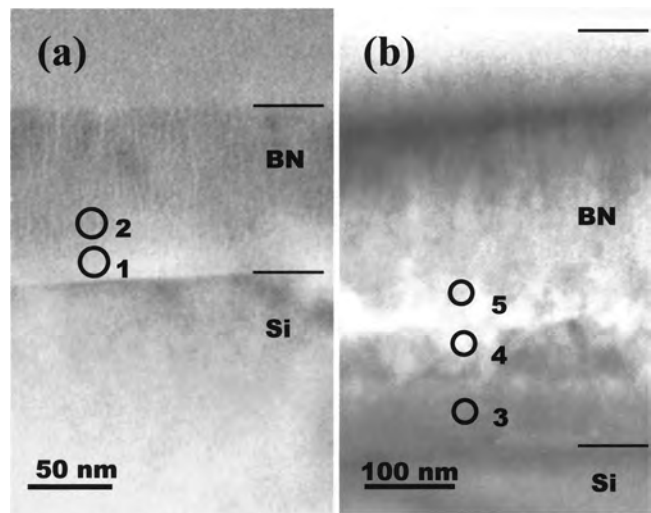


FIG. 2. Low magnification TEM images of BN film (a) and (b) types grown at the -120 and -50 V bias.

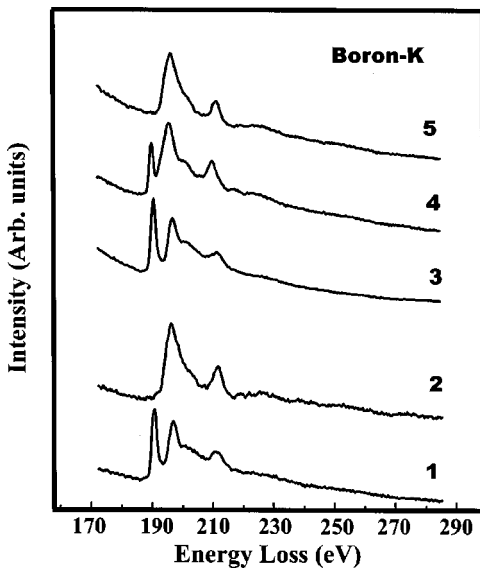


FIG. 3. EELS spectra of films (a) and (b) taken from different areas of each film. The spectra 1–2 and 3–6, as denoted in Fig. 2, were collected from the films types (a) and (b), respectively.

substrate interface as designed the area 5 and above, are similar to that taken from the area 2 in the film type (a), indicating that the BN phase in the film type (b) above the area 5 is again $\sim 100\%$ *c*-BN.

The TEM results of the film type (a) are similar to those well reported in the literature.^{14,15} They are described for comparison with the data of the film type (b). Figure 4(a) shows a TED pattern taken at the interface of the film (a) and the substrate with the electron beam oriented along the Si [110] direction. The *t*-BN (0002) diffraction spots are measured to be 90° away from the Si (002) diffractions. However, instead of uniform ring patterns, three incomplete rings consisting of several elongated spots and corresponding to the *c*-BN (111), (220), and (311) diffractions are observed, respectively. The diffraction pattern of the film type (a) indicates preferential orientations in both *t*-BN and *c*-BN phases. These observations are further supported by the high-resolution images taken at the BN/Si interface as well as the *c*-BN/*t*-BN interface with electron beam oriented along the Si (110) zone axis. Figure 5(a) shows that an amorphous BN layer is first formed on the Si substrate, followed by an oriented *t*-BN layer, with its (0002) planes perpendicular to the Si surface. The basal plane spacing in the *t*-BN layer is 3.6 Å, slightly larger than that of hexagonal BN (*h*-BN). The edges of the *t*-BN (0002) planes are aligned to the film growth direction. Figure 6(a) shows that the *c*-BN nucleates on the edges of the *t*-BN (0002) planes and further grows with its (111) planes parallel to the *t*-BN (0002) planes. A 3:2 (*c*-BN:*t*-BN) lattice match is maintained locally.

Figure 4(c) shows the TED pattern taken at the interface of the film (b) and the substrate. The diffractions from *t*-BN (0002) planes are elongated form spots to arclike pattern, almost close up to a ring with stronger intensity along the direction perpendicular to the Si (002) diffraction. This indicates that the preferential orientation in the *t*-BN layer diminished to a large extent. The three relatively uniform rings

correspond to the *c*-BN (111), (220), and (311) diffractions, respectively. The uniformity of the ring pattern indicates that the *c*-BN crystallites are randomly oriented. The random orientation of the *t*-BN is further confirmed by the high-resolution images taken at the BN/Si interface with electron beam oriented along the Si (110) zone axis. Figure 5(b) shows that *t*-BN layer on top of a thin *a*-BN layer no longer has its (0002) planes perpendicular to the substrate surface, but is growing in different directions. Some *t*-BN (0002) planes with large curvatures are formed and the edges of the *t*-BN (0002) planes are no longer aligned to the growth direction due to the random orientation of the curved basal planes. Figure 6(b) is a high-resolution image taken at the interface of *t*-BN and *c*-BN. A curled (0002) plane of *t*-BN is exposed along the growth direction and *c*-BN is observed to nucleate on the curved *t*-BN plane and further grow. The (111) planes of *c*-BN are no longer parallel to the *t*-BN (0002) planes due to the curved nature of the *t*-BN planes. Note also that while in film (a) the *c*-BN planes are approximately parallel to the growth direction, this is not the case any more for the *c*-BN growing on curled *t*-BN planes.

Two other samples, film (x1) and film (x2), were deposited using substrate biases of -100 and -80 V, while other deposition parameters were kept the same as in the case of the film types (a) and (b). The HRTEM (not shown here) and TED data [Fig. 4(b)] of these films is intermediate between the films (a) and (b). Table I summarizes the variations of the film properties with altering the substrate bias within a range of -120 to -50 V. As the substrate bias changes from -120 to -50 V, the internal stress of the film decreases from ~ 11 to ~ 4.5 GPa though the maximum film thickness before delamination increases from 100 to 500 nm. The thickness of the *t*-BN layer increases from ~ 25 to ~ 150 nm as the substrate bias decreases. This explains the increase in *t*-BN fraction of the film as a whole, while the BN layer on top of it remains $\sim 100\%$ *c*-BN. Both types of *c*-BN nucleation environments, i.e., the “edge nucleation” (type I) and “curvature nucleation” (type II), are observed for all these films. The fraction of the type II nucleation, however, increases from ~ 0 to $\sim 30\%$ as the substrate bias decreases. XPS confirmed that the B/N ratio remains close to unity for all these films. The -50 V bias voltage is very close to the threshold value of *c*-BN formation under current experimental conditions. A further decrease of the bias below -50 V suppresses the *c*-BN growth.

IV. DISCUSSION

The growth of *c*-BN involves several distinct stages, in each of which different mechanisms occur. These stages include (1) *a*-BN formation, (2) *t*-BN formation, (3) *c*-BN nucleation, and (4) *c*-BN growth (and renucleation).

For BN film deposited at a high substrate bias, the transition from the first to the second stage of the growth may be explained by two ways: (i) the stress model and (ii) the preferential displacement model. The stress argument claims that the preferred orientation in the *t*-BN layer is considered to result from the compressive stress induced by the ion bombardment. McKenzie and co-workers^{1,8,16,17} consider the

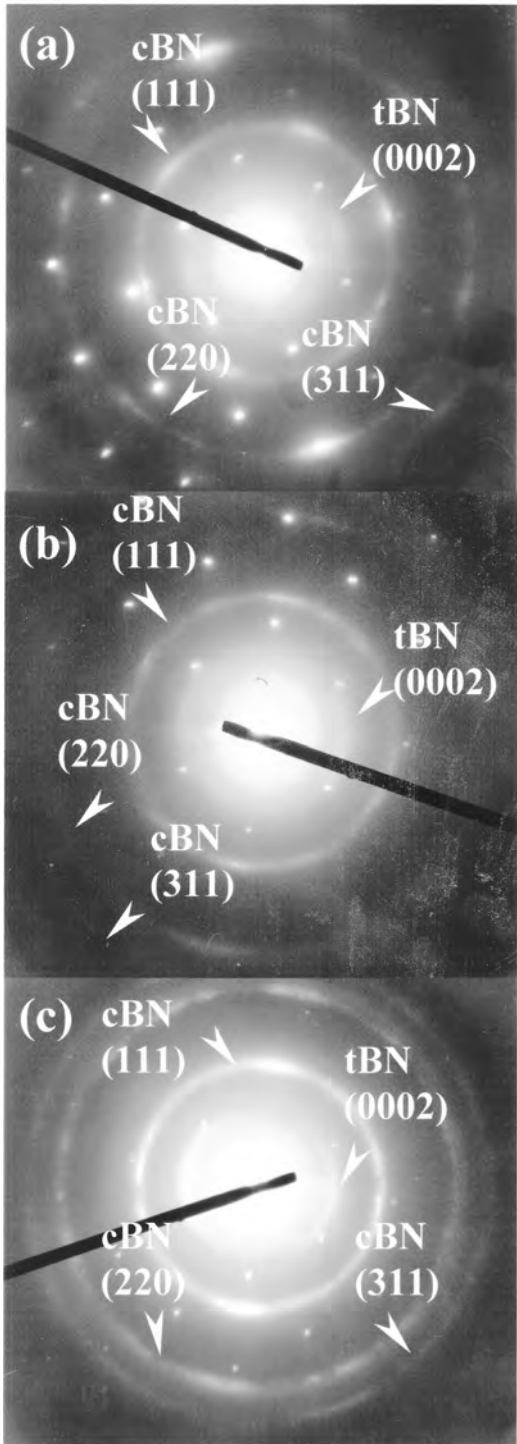


FIG. 4. TED patterns of BN films (a) [Fig. 4(a)], (x2) [Fig. 4(b)] and (b) [Fig. 4(c)] (substrate biases of -120 , -80 , and -50 V, respectively). For the film (a) [Fig. 4(a)], the two t -BN (0002) diffraction spots are perpendicular to the Si(002) spots indicating an oriented t -BN growth; the incomplete diffraction ring of c -BN indicates that the c -BN crystallites are preferentially oriented. For the film (b) [Fig. 4(c)], the diffraction from both the t -BN (0002) planes and the c -BN form ringlike patterns indicating a significant component of randomly oriented t -BN and c -BN. For the film (x2) the TED pattern [Fig. 4(b)] is intermediate between those of the films (a) and (b).

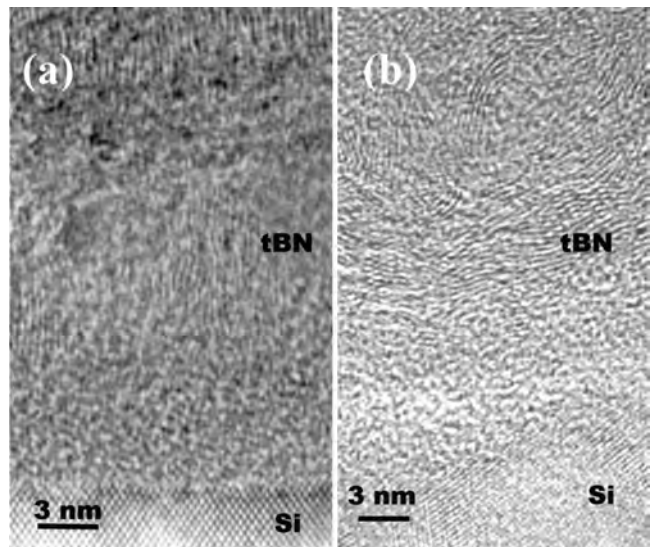


FIG. 5. High-resolution TEM images of film (a) and (b) taken at the interface of the BN film and silicon substrate with the electron beam oriented along the Si[110] direction.

thermodynamics of the system and find that the preferred orientation where the t -BN basal layers are arranged in the most compressible way (c axis parallel to the surface along the biaxial stress direction) has the lowest Gibbs free energy. Cardinale *et al.*¹⁸ claim that the plastic deformation of the BN, rather than the minimum elastic strain energy contributes to the observed orientation of the t -BN basal planes, as their energy calculation shows that the most favorable orientation would be a 45° tilt of the t -BN basal planes from the substrate surface. Lifshitz and co-workers^{19–21} suggested an alternative explanation for the ion-induced orientation of carbon films: preferential displacement of atoms in the direction perpendicular to the basal planes (C-C bond energy ~ 0.8 eV) with respect to the displacements in the plane (bond energy 7.4 eV). It is interesting to point out that Kulik and co-workers^{20,21} indeed found a compression in oriented graphitic layers grown at elevated substrate temperatures (the spacing between the planes is smaller by 5% with respect to graphite), in accord with a stress induced mechanism. However, the reported spacing of the t -BN layers is 5–15% larger than that of crystalline h -BN,¹ in accord with our present work, similar to the carbon films obtained by Lifshitz *et al.* for high-energy (20 keV), room-temperature depositions.²¹ This may indicate the significance of the preferential displacement in the orientation of the t -BN layers rather than the role of compressive stress, which should lead to smaller spacing of the basal planes with respect to the hexagonal phase rather than the observed larger spacings. A compressive stress associated with lined-up t -BN (0002) planes with a larger spacing than for h -BN can be explained by the formation of t -BN nanotubes with the tube axis along the growth direction. In fact, the formation of carbon nanotubes has actually been reported during direct ion beam deposition of diamondlike carbon films.²¹ For BN films deposited at lower bias (lower ion energy), the formation of curled t -BN planes with random orientation reported here may be either due to a smaller amount of displacements or owing to con-

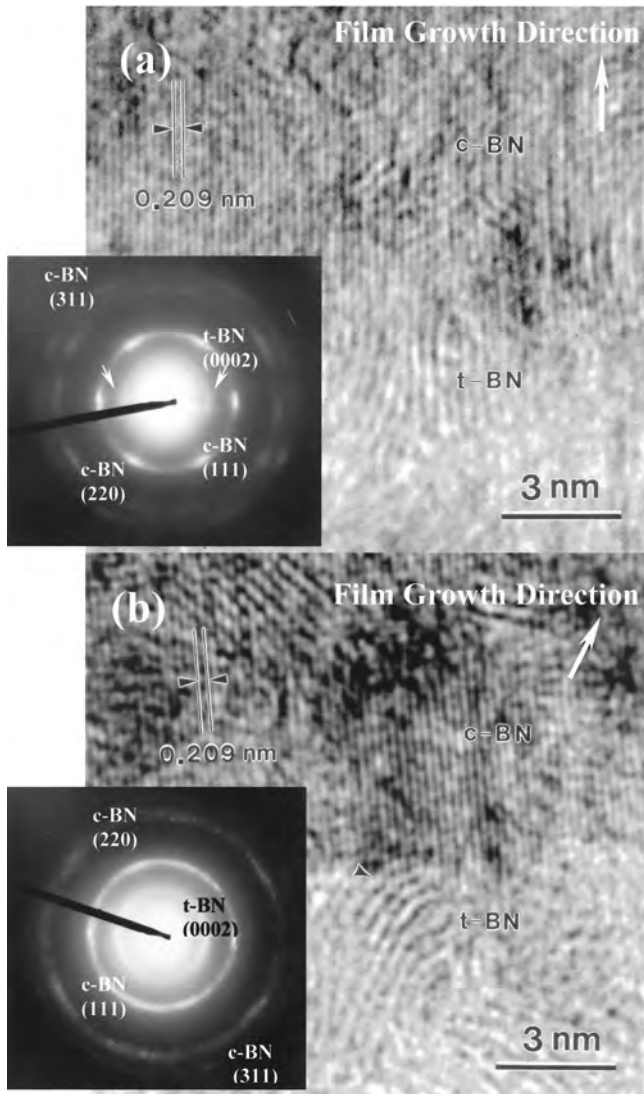


FIG. 6. High-resolution TEM images of the film (a) and (b) taken at the *t*-BN/*c*-BN interface with characteristic diffraction patterns shown in insets. Note the arrows indicating the growth direction. For (a) the *c*-BN (111) planes growth is parallel to the growth direction, which is not the case for (b).

ditions favoring reorganization to the minimal Gibbs free energy state (as suggested by Cardinale *et al.*¹⁸). However, in both cases it is unclear whether the significant stress observed in the films already exists in the *t*-BN layer or only

evolves later in the subsequent *c*-BN layer.

Until now we have only dealt with the formation of the *t*-BN layer. The next growth stage of our films is the nucleation of *c*-BN crystallites on top of *t*-BN layers. In the high bias case, experimental observation suggests that the edges of the (0002) planes provide nucleation sites for the formation of the cubic phase. The orientation relation between the two is associated with the local geometrical similarity and the close 2:3 match between the *t*-BN (0002) spacing (3.33 Å) and the *c*-BN (111) spacing (2.06 Å).^{1,13,21,22} Lambrecht *et al.*^{22,23} showed that the interface between the *c*-BN (cubic diamond) crystallites and *h*-BN (graphite) with that specific geometric configuration is energetically favorable. Both the matching of the *t*-BN (0002) and *c*-BN (111) layers and the energetically favorable configuration of the interface between those layers indicate that *t*-BN can serve as a nucleation site for *c*-BN growth. In the lower bias case, another type of nucleation site, i.e., curved (0002) planes, was observed in the present work. This nucleation site coexists with the one described above. It is generally understood that planar *t*-BN (0002) planes do not allow *c*-BN nucleation. As the saturated *sp*² B-N bonding is already formed for this configuration, no active site would be available along the growth direction. The bending of the *t*-BN planes makes it possible for dangling bonds of either B or N to stick out and serve as a nucleation site for the cubic phase. A recent COSDAF Si nanowire study indicates a similar trend: SiH₃ forms much more readily on Si nanowires than on a bulk Si surface.²⁴ In fact, Collazo-Davila *et al.*,^{12,25} who studied BN nanoarches, have speculated that the curling *sp*² structures might serve as *c*-BN nucleation sites due to the *sp*³ character of B-N-B bonds in curled *sp*² bonded sheets. The present work is in accord with their speculation, for which they did not provide experimental evidence.

We can now address the next stage, i.e., the formation and growth of *c*-BN nuclei on the nucleation sites and the further growth of the *c*-BN films. The conditions necessary for the formation of critical cubic nuclei (*c*-BN or cubic diamond) on a specific nucleation site are still unclear and the different mechanisms¹ suggested (sputter, stress, thermal spike, subplantation) are still speculative and need further substantiation. The new nucleation environment (curled *t*-BN) leads to a randomly oriented growth of the *c*-BN with respect to the *t*-BN layers or the initial substrate, contrary to the oriented *c*-BN growth on the edge of the *t*-BN (0002) planes. The oriented *c*-BN growth on top of the *t*-BN (0002) plane edges

TABLE I. Variation of boron nitride properties upon altering the substrate bias.

Substrate Bias (V)	Internal stress of the film (GPa)	Total film thickness at delamination (nm)	<i>t</i> -BN layer thickness (nm)	Fraction of the type II <i>t</i> -BN/ <i>c</i> -BN environment (%)
Film (a)	~120	~11	~100	~25
Film (x1)	~100	~9	~150	~40
Film (x2)	~80	~6	~300	~100
Film (b)	~50	~4.5	~500	~150

[*c*-BN (111)//*t*-BN (0002)] is in accord with the match between these planes. Three *c*-BN (111) planes match two *t*-BN planes (the ratio between the plane spacings is 2:3). When viewed normal to these planes both the *c*-BN and *t*-BN atoms form identical six membered rings (hexagons), the *t*-BN rings flat and the *c*-BN rings puckered. This oriented *c*-BN growth is associated with a significant stress buildup. It is unclear at present whether the oriented growth is stabilized by the stress (similar to the oriented *t*-BN growth) or it is a pure geometrical effect. The stress itself could be resulting from the oriented growth rather than the origin of the oriented growth. An indication for a reduction in stress by lowering the bias towards the threshold energy has been suggested by Hofsäss *et al.*²⁶ by relating the IR peak to the stress. The lack of orientation between the curled *t*-BN sites and the *c*-BN sites may be the result of the lack of a geometrical match between the *t*-BN and *c*-BN for this nucleation environment allowing a nonoriented *c*-BN growth. The association of the stress buildup to the oriented *c*-BN growth rather than the ion impact indicates that the nonoriented *c*-BN growth would lead to low stress levels if any. Matsumoto *et al.*²⁷ indeed report the formation of thick, nearly stress free *c*-BN films which we found to be randomly oriented (using HRTEM), in accord with the present work.

Our gradual change of the bias during BN growth enabled us to control the relative amount of the two types of nucleation [type I: (0002) *t*-BN plane edges and type II: curled (0002) *t*-BN planes] within the range of ~0–30% relative amount of type II. Table I shows that a thicker layer of *t*-BN is needed for *c*-BN nucleation as the amount of type II sites increase. Since the availability of nucleation sites does not depend on the *t*-BN thickness this indicates that the nucleation necessitates an additional factor, most likely an integral stress buildup. If the local stress in the *t*-BN layer decreases with the reduction of the bias a thicker *t*-BN layer would be needed to achieve the critical integral stress required for *c*-BN nucleation. The experimental evidence presented in Table I suggests that the stress buildup in *c*-BN films is associated with the growth of oriented *c*-BN layers on the oriented (0002) *t*-BN edges. Reduction of the amount of the type I *c*-BN decreases the stress generated in the films so that thicker *c*-BN films can be deposited without delamination. Until now the films deposited by us contained a mixture of *c*-BN crystallites grown on the two types of nucleation sites with a maximal fraction of the second type of ~30%. This means that our films still contain a significant amount of stress originating from the large component of type I *c*-BN. The type II BN fraction indeed increases as the substrate bias drops. Although a thicker *t*-BN layer growth is associated

with the bias decrease, the *c*-BN layer on top of it remains ~100% pure, thus guaranteeing the film quality. It is reasonable to assume that by optimizing our deposition conditions to acquire only the second type of *c*-BN crystallites we could remove the stress generated in *c*-BN layers and be able to deposit thick *c*-BN films. The –50 V bias voltage is very close to the energy limit of *c*-BN growth. The *c*-BN nucleation is sensitive to the change in bias in the vicinity of this threshold voltage. The bias voltage threshold for *c*-BN nucleation may also change with the ion-to-atom ratio, as well demonstrated in the literature.¹ This means that several parameters may be tuned to control the nucleation environment and reduce the stress associated with the *c*-BN growth. It should also be noted that once the nucleation starts, the bias necessary for further *c*-BN growth might be further reduced (i.e., the nucleation conditions are different than the growth conditions) which might further reduce the *c*-BN stress and still increase the maximal obtainable *c*-BN thickness. We would also like to point out that previous attempts^{8–10} to reduce the stress and grow thicker *c*-BN films involved deposition temperatures much higher than that applied in the present work (1000 °C compared to 450 °C). High-temperature annealing may be the cause of this reported stress relief rather than the reduced bias. The low-temperature stress relief reported here may be advantageous for practical applications.

V. SUMMARY

We report a type of *t*-BN growth in addition to the oriented *t*-BN growth generally reported in energetically deposited BN films. It serves as a different nucleation environment for *c*-BN, i.e., *c*-BN nucleates on the curved planes of *t*-BN and further grows without any specific orientation to the *t*-BN, contrary to the *c*-BN nucleation and oriented growth on the edges of (0002) *t*-BN planes. We have shown that nonoriented growth of *t*-BN and *c*-BN is associated with low stress levels and thus facilitates the production of thicker films. The fraction of different *t*-BN/*c*-BN environments can be controlled and varied by changing the substrate bias during film deposition. Both growth types require a UHV base pressure since O is detrimental to *c*-BN growth. These findings give additional insight and increase our understanding of the *c*-BN growth mechanisms and may be optimized for the formation of thick, possibly stress free *c*-BN films.

ACKNOWLEDGMENTS

This work was funded by the RGC of Hong Kong under Grant No. 9040 292.

*On leave from Department of Material Science & Engineering, Northwestern University, Evanston, IL 60208.

[†]On leave from Soreq NRC, Yavne 81800, Israel.

[‡]Corresponding author. E-mail address: apibello@cityu.edu.hk

¹P. B. Mirkarimi, K. F. McCarty, and D. L. Medlin, Mater. Sci. Eng., R. **21**, 47 (1997).

²D. J. Kester, K. S. Ailey, R. F. Davis, and K. L. More, J. Mater.

Res. **8**, 1213 (1993).

³G. F. Cardinale, P. B. Mirkarimi, K. F. McCarty, E. J. Klaus, D. L. Medlin, W. M. Clift, and D. G. Howitt, Thin Solid Films **253**, 130 (1994).

⁴S. Reinke, M. Kuhr, W. Kulisch, and R. Kassing, Diamond Relat. Mater. **4**, 272 (1995).

⁵S. Watanabe, S. Miyake, W. Zhou, Y. Ikuhara, T. Susuki, and M.

- Murakawa, Appl. Phys. Lett. **66**, 1478 (1995).
- ⁶T. Yoshida, Diamond Relat. Mater. **5**, 501 (1996).
- ⁷D. L. Medlin, T. A. Friedmann, P. B. Mirkarimi, G. F. Cardinale, and K. F. McCarty, J. Appl. Phys. **79**, 3567 (1996).
- ⁸D. R. McKenzie, W. D. McFall, S. Reisch, B. W. James, I. S. Falconer, R. W. Boswell, H. Persing, A. J. Perry, and A. Durander, Surf. Coat. Technol. **78**, 255 (1996).
- ⁹J. Hahn, F. Richter, R. Pintaske, M. Roder, E. Schneider, and T. Welzel, Surf. Coat. Technol. **92**, 129 (1996).
- ¹⁰D. Litvinov and R. Clarke, Appl. Phys. Lett. **71**, 1969 (1997).
- ¹¹Z. F. Zhou, I. Bello, M. K. Lei, K. Y. Li, C. S. Lee, and S. T. Lee, Surf. Coat. Technol. **128–129**, 334 (2000).
- ¹²C. Collazo-Davila, E. Bengu, C. Leslie, and L. D. Marks, Appl. Phys. Lett. **72**, 314 (1997).
- ¹³A. J. Perry, J. A. Sue, and P. J. Martin, Surf. Coat. Technol. **81**, 17 (1996).
- ¹⁴M. P. Johansson, L. Hultman, S. Daaud, K. Bewilogua, H. Luthje, A. Schutze, S. Kouptsidas, and G. S. A. M. Theunissen, Thin Solid Films **287**, 193 (1996).
- ¹⁵W. L. Zhou, Y. Ikuhara, and T. Suzuki, Appl. Phys. Lett. **67**, 3551 (1995).
- ¹⁶D. R. McKenzie, D. J. H. Cockayne, D. A. Muller, M. Murakawa, S. Miyake, S. Wantanabe, and P. Fallon, J. Appl. Phys. **70**, 3007 (1991).
- ¹⁷D. R. Mckenzie, W. D. McFall, W. G. Sainty, C. A. Davis, and R. E. Collins, Diamond Relat. Mater. **2**, 970 (1993).
- ¹⁸G. F. Cardinale, D. L. Medlin, P. B. Mirkarimi, K. F. McCarty, and D. G. Howitt, J. Vac. Sci. Technol. A **15**, 196 (1997).
- ¹⁹Y. Lifshitz, S. R. Kasi, J. W. Rabalais, and W. Eckstein, Phys. Rev. B **41**, 10 468 (1990).
- ²⁰J. Kulik, G. Lempert, E. Grossman, and Y. Lifshitz, *Proceedings of MRS 1999 Fall Meeting*, MRS Symposia Proceedings No. 593 (Materials Research Society, Pittsburgh, 2000).
- ²¹Y. Lifshitz, J. Kulik, H. Y. Peng, and S. T. Lee, Phys. Rev. Lett. (to be published).
- ²²W. R. L. Lambrecht, C. H. Lee, B. Segall, J. C. Angus, Z. Li, and M. Sunkara, Nature (London) **364**, 607 (1993).
- ²³J. Widany, T. Frauenheim, and W. R. L. Lambrecht, J. Mater. Chem. **6**, 899 (1996).
- ²⁴D. D. Ma, C. S. Lee, F. C. K. Au, S. Y. Tong, and S. T. Lee (unpublished).
- ²⁵C. Collazo-Davila, E. Bengu, L. D. Marks, and M. Kirk, Diamond Relat. Mater. **8**, 1091 (1999).
- ²⁶H. Hofsäss, H. Feldermann, M. Sebastian, and C. Ronning, Phys. Rev. B **55**, 13 230 (1997).
- ²⁷S. Matsumoto and W. J. Zhang, Jpn. J. Appl. Phys. **39**, L442 (2000).